Nonlinear Analysis: Real World Applications 13 (2012) 64–77

Contents lists available at SciVerse ScienceDirect

Nonlinear Analysis: Real World Applications

journal homepage: www.elsevier.com/locate/nonrwa

Bifurcation analysis in a model of cytotoxic T-lymphocyte response to viral infections

Bernard S. Chan *, Pei Yu

Department of Applied Mathematics, University of Western Ontario, London, Ontario, Canada N6A 5B7

ARTICLE INFO

Article history:
Received 23 April 2010
Accepted 16 July 2011

Keywords:
Immune system
Cytotoxic T-lymphocyte response
Hopf bifurcation
Stability
Limit cycles

ABSTRACT

In this paper, we study the dynamics of a mathematical model on primary and secondary cytotoxic T-lymphocyte (CTL) response to viral infections by Wodarz et al. This model has three equilibria and their stability criteria are discussed. The system transitions from one equilibrium to the next as the basic reproductive number, R_0, increases. When R_0 increases even further, we analytically show that periodic solutions may arise from the third equilibrium via Hopf bifurcation. Numerical simulations of the model agree with the theoretical results and these dynamics occur within biologically realistic parameter range. The normal form theory is also applied to find the amplitude, phase and stability information on the limit cycles. Biological implications of the results are discussed.

1. Introduction

From the advances in immunology over the past few decades, we are now able to understand the dynamics of infections at the cellular level. This detailed level of understanding allows researchers to simulate the interactions between pathogens and the host immune system using computer models. Of the many different mechanisms of the immune system, defenses against viral infections are of interest because many of the diseases caused by them, e.g. hepatitis B and AIDS, are chronic and incurable [1,2].

A virus cannot replicate on its own and it must take over host cells and use them in order to replicate. Once invaded by the viruses, these infected cells will cause a cytotoxic T-lymphocyte (CTL) response from the immune system. Cells involved in the CTL response are also known as killer T-cells because they are responsible for apoptosis, i.e., programmed cell death, of the infected cells. Through the lysis of the infected cells, the viruses are prevented from further replication [2]. The CTL response is also notable because it sometimes damages the body in its attempt to clear the virus. Over half the tissue damage in hepatitis is actually caused by the CTL response [1,3].

To model the immune response during a viral infection, researchers first consider the basic interactions between the immune system and the virus using the following system of differential equations [4,5]:

$$\begin{aligned} \dot{x} &= \lambda - dx - \beta x v, \\ \dot{y} &= \beta x v - a y, \\ \dot{v} &= k y - \mu v, \end{aligned} \tag{1}$$

where variables x, y and v represent the density of the healthy cells, the infected cells, and the virus, respectively. Healthy cells are produced at rate λ and they died out naturally at rate dx. These cells may come into contact with the virus and

* Corresponding author.
E-mail addresses: bchan6@uwo.ca (B.S. Chan), pyu@uwo.ca (P. Yu).

1468-1218/$ – see front matter © 2011 Elsevier Ltd. All rights reserved.
doi:10.1016/j.nonrwa.2011.07.012

become infected cells at rate βxv. Infected cells died out naturally at rate ay. From the infected cells, the viruses are replicated at rate ky and they are cleared naturally at rate μv.

To recover from a viral infection, cytotoxic T-lymphocyte effectors (CTLe) of the immune system will clear away the infected cells to prevent further viral replications. To model these extra dynamics, researchers modified model (1) by assuming that the virus population is at a quasi-steady state, i.e. $v = (k/\mu)y$, and let z represent the CTLe population to get a simple model of viral interaction with CTL response [5,6]:

$$\begin{aligned} \dot{x} &= \lambda - dx - \beta xy, \\ \dot{y} &= \beta xy - ay - pyz, \\ \dot{z} &= cyz - bz. \end{aligned} \tag{2}$$

Compared to model (1), healthy cells in this model become infected cells at rate βxy and the infected cells are removed by z at pyz. The CTL population increases nonlinearly at rate cyz and they are removed at rate bz.

After a viral infection, the CTLs that were responsible for clearing away the infected cells become cytotoxic T-lymphocyte precursors (CTLp) and they have receptors specifically for detecting the virus from the previous infection [3]. Upon contact with the virus during a subsequent infection, the precursors differentiate and become cytotoxic T-lymphocyte effectors (CTLe) and these cells are again responsible for clearing away the invading virus. Hence, the following model from [7] more accurately describes the dynamics of CTL response in the immune system:

$$\begin{aligned} \dot{x} &= \lambda - dx - \beta xy \\ \dot{y} &= \beta xy - ay - pyz \\ \dot{w} &= cyw - cqyw - bw \\ \dot{z} &= cqyw - hz. \end{aligned} \tag{3}$$

For this system, the healthy cells, x, and the infected cells, y, are described similarly as in system (2). Instead of just one class of CTL response, there are the CTLp represented by w and the CTLe represented by z. These precursors emerge at rate cyw. They may become effectors at rate $cqyw$ or cleared away naturally at rate bw. Similarly, the effectors are created at rate $cqyw$ and cleared at rate hz.

Dynamics of system (3) was analyzed mostly by numerical methods in [7]. In this study, we provide a rigorous analysis of system (3) similar to those done in [8,9]. To start, we show that the system is a well-posed biological model in Section 2. Local analysis of equilibria for system (3) was partially carried out in [7], so we complete the local as well as the global stability analysis in Section 3. Aside from stability, we will analyze bifurcation dynamics using conditions established by Yu [10] in Section 4.2. We provide some numerical illustrations to the system in Section 5. Finally, the biological significance of the results are discussed in Section 6.

2. Well-posedness of the model

For a biological model to be well-posed, only non-negative initial conditions are considered and the solution must not be negative. Let the parameters in (3) be positive constants. Directly solving for x, the solution is

$$x(t) = \mathrm{e}^{-\int_0^t (d+\beta y(s))\mathrm{d}s} x(0) + \lambda \int_0^t \mathrm{e}^{-\int_s^t (d+\beta y(u))\mathrm{d}u} \mathrm{d}s.$$

For $t > 0$ and $x(0) \geq 0$, one can see that $x(t) > 0$. In a similar fashion, we can show that the other three variables have solutions as

$$\begin{aligned} y(t) &= y(0)\mathrm{e}^{\int_0^t [\beta x(s) - a - pz(s)]\mathrm{d}s}, \\ w(t) &= w(0)\mathrm{e}^{\int_0^t [cy(s)(1-a) - b]\mathrm{d}s}, \\ \text{and} \quad z(t) &= \mathrm{e}^{-ht}\left(z(0) + \int_0^t cqy(s)w(s)\mathrm{e}^{hs}\mathrm{d}s\right). \end{aligned}$$

All solutions are positive for $t > 0$ if $y(0) > 0$, $w(0) > 0$, and $z(0) \geq 0$.

Aside from positivity, boundedness is another criteria for a well-posed biological model. Given that the exponential functions have negative exponents, we show that $x(t)$ for $t > 0$ is bounded by

$$\begin{aligned} x(t) &< \mathrm{e}^{-\int_0^t d\,\mathrm{d}s}\left(x(0) + \lambda \int_0^t \mathrm{e}^{-\int_s^t d\,\mathrm{d}u}\mathrm{d}s\right) \\ &= \mathrm{e}^{-\mathrm{d}t}\left(x(0) + \lambda \int_0^t \mathrm{e}^{-d(t-s)}\mathrm{d}s\right) \\ &= \mathrm{e}^{-\mathrm{d}t}\left(x(0) + \frac{\lambda}{d}\left(1 - \mathrm{e}^{-\mathrm{d}t}\right)\right). \end{aligned}$$

Combining the boundedness of $x(t)$ and the positivity of $z(t)$, one can see that the integrand in $y(t)$ must also be bounded. Since the integrand is bounded, $y(t)$ must be bounded for $t > 0$. Using the same boundedness argument for $y(t)$, we can show that $w(t)$ is also bounded. For $z(t)$, we know that $z(0)\mathrm{e}^{-ht}$ is bounded. As for the other part of the solution, it may be unbounded as $t \to \infty$. We apply l'Hopital's rule to get

$$\lim_{t\to\infty} \mathrm{e}^{-ht} \int_0^t cqy(s)w(s)\mathrm{e}^{hs}\mathrm{d}s \overset{\mathrm{H}}{=} \lim_{t\to\infty} \frac{cqy(t)w(t)\mathrm{e}^{ht}}{h\mathrm{e}^{ht}} = \frac{cqy(\infty)w(\infty)}{h}.$$

By the boundedness of $y(t)$ and $w(t)$, $z(t)$ is also bounded. Hence, we have shown system (3) to be a well-posed biological model.

First, we discuss the stability of E_0 and E_1 and their bifurcation. In the next section, we will discuss the stability of E_2 and Hopf bifurcation. For system (3), the three equilibria are given by

$$E_0 = \left(\frac{\lambda}{d}, 0, 0, 0\right), \tag{4}$$

$$E_1 = \left(\frac{a}{\beta}, \frac{\lambda\beta - da}{a\beta}, 0, 0\right), \quad \text{and} \tag{5}$$

$$E_2 = \left(\frac{\lambda}{dR_1}, \frac{b}{cQ}, \frac{h}{pqbcd}\left(\frac{R_0}{R_1} - 1\right), \frac{1}{pcdQ}\left(\frac{R_0}{R_1} - 1\right)\right), \tag{6}$$

where

$$Q = (1 - q),$$
$$R_0 = \frac{\lambda\beta}{ad},$$
$$\text{and} \quad R_1 = 1 + \frac{\beta b}{cdQ}.$$

The stability of the equilibria is based on the Jacobian matrix of (3):

$$J(x, y, w, z) = \begin{bmatrix} -d - y\beta & -\beta x & 0 & 0 \\ y\beta & -\beta x - a - pz & 0 & -py \\ 0 & cw(1-q) & cy(1-q) - b & 0 \\ 0 & cqw & cqy & -h \end{bmatrix}. \tag{7}$$

3. Stability of E_0 and E_1

3.1. Infection-free equilibrium E_0

By the way of (7), we obtain the characteristic polynomial at the equilibrium E_0 as follows.

$$\Lambda_{E_0}(s) = \det[\lambda I - J(E_0)] = (s + d)(s + b)(s + h)\left(s + a - \frac{\beta}{d}\right).$$

For an equilibrium to be locally asymptotically stable, all the roots of the characteristic polynomial must be located in $\mathbb{C}^- = \{z \in \mathbb{C} : \mathrm{Re}(z) < 0\}$. Given that all the parameters of the system are positive, the system is locally asymptotically stable at this equilibrium if

$$\lambda\beta - da < 0 \quad \text{or} \quad R_0 \triangleq \frac{\lambda\beta}{ad} < 1,$$

where R_0 represents the basic reproductive number.

To show that this equilibrium is globally stable, we will follow the method of fluctuation employed by Hirsch et al. [11] and Jiang et al. [8]. To start, we denote

$$f_\infty = \liminf_{t\to\infty} f(t) \quad \text{and} \quad f^\infty = \limsup_{t\to\infty} f(t)$$

for any continuous and bounded function $f : [0, \infty) \to \mathbb{R}$. As shown in Section 2, the solutions $x(t)$, $y(t)$, $w(t)$, and $z(t)$ are always non-negative and bounded from above for any well-posed initial conditions. Hence, $\liminf_{t\to\infty}$ and $\limsup_{t\to\infty}$ always exist for each component. By the theorems on fluctuations [12], there exists a sequence t_n such that if $t_n \to \infty$ whenever $n \to \infty$, then

$$\lim_{n\to\infty} x(t_n) = x^\infty \quad \text{and} \quad \lim_{n\to\infty} \dot{x}(t_n) = 0. \tag{8}$$

Suppose $t = t_n$, then the first equation from system (3) gives

$$\dot{x}(t_n) + dx(t_n) + \beta x(t_n)y(t_n) = \lambda.$$

As $n \to \infty$, one can apply identities in (8) and the previous equation becomes

$$dx^\infty \le (d + \beta y_\infty)x^\infty \le \lambda. \tag{9}$$

By similar arguments on the other equations in system (3), we have

$$ay^\infty \le (a + pz_\infty)y^\infty \le \beta x^\infty y^\infty, \tag{10}$$

$$bw^\infty \le c(1-q)y^\infty w^\infty, \tag{11}$$

$$\text{and} \quad hz^\infty \le cqy^\infty w^\infty. \tag{12}$$

Now, we can derive from Eqs. (9) and (10) to get

$$ay^\infty \le \beta x^\infty y^\infty \le \frac{\lambda\beta}{d} y^\infty. \tag{13}$$

Suppose $y^\infty > 0$, inequality (13) implies

$$1 \le \frac{\lambda\beta}{ad} = R_0,$$

which contradicts $R_0 < 1$, and so $y^\infty = 0$. Given $y^\infty = 0$, Eqs. (11) and (12) imply that $w^\infty = 0$ and $z^\infty = 0$. Since the solutions are non-negative and $\liminf \le \limsup$, we must have $y(t), w(t), z(t) \to 0$ as $t \to \infty$. Because $y(t) \to 0$ asymptotically, the first equation in (3) becomes $\dot{x} = \lambda - dx$. Similar to the results in [13], the solution $x(t) \to \lambda/d$ as $t \to \infty$. By the local stability result established earlier and the global attractive property shown here, we have proven the following theorem.

Theorem 1. *When $R_0 < 1$, the infection-free equilibrium E_0 is globally asymptotically stable.*

3.2. Infectious equilibrium without CTL response E_1

When $R_0 > 1$, E_0 becomes unstable and a new equilibrium E_1 emerges. For this equilibrium solution to be physically meaningful, we must have $R_0 > 1$. Similarly, with the aid of (7) the characteristic equation at E_1 can be obtained as

$$\begin{aligned}\Lambda_{E_1}(s) &= \det[\lambda I - J(E_1)] \\ &= \frac{1}{a^2\beta}(s+h)(as^2 + \lambda\beta s + \beta\lambda a - da^2)\left[a\beta s + cQ(ad - \beta\lambda) + a\beta b\right].\end{aligned}$$

There are two first-degree factors and one second degree factor. Given that all the parameters are positive, the first root is obviously stable. For the roots of the second-degree factor to be in $\mathbb{C}^-$, all its coefficients must have the same sign. Hence, its roots would be stable if and only if $R_0 > 1$. This condition is same as the condition for the equilibrium to be biologically meaningful, so we only need to check the remaining root. This equilibrium is locally stable if and only if

$$\begin{aligned}cQ(ad - \beta\lambda) + a\beta b > 0 &\Leftrightarrow cdQ(R_0 - 1) - \beta b < 0 \\ &\Leftrightarrow R_0 - 1 - \frac{\beta b}{cdQ} < 0, \\ &\Leftrightarrow R_0 < 1 + \frac{\beta b}{cdQ} \triangleq R_1.\end{aligned}$$

Not only that the system is locally stable at this equilibrium, one can show that this equilibrium is globally stable.

Theorem 2. *When $1 < R_0 < R_1$, the infectious equilibrium without CTL response is globally asymptotically stable.*

Proof. To prove that the system is globally asymptotically stable, we will use the Lyapunov stability theory to show that the system must converge to a region in hyperspace and upon entering such region, the solutions must converge to the equilibrium asymptotically. Based on the Lyapunov function candidates suggested in [14], we investigate the system using

$$V(x, y, w, z) = m\left(x - x_1 - x_1 \ln\frac{x}{x_1} + y - y_1 - \ln\frac{y}{y_1}\right) + \tilde{m}(w + z),$$

where m as well as $\tilde{m}$ are positive coefficients yet to be determined, and x_1 as well as y_1 are the equilibrium expressions of x and y at E_1. Clearly, $V(E_1) = 0$, which is the unique global minimum of the function. Now, we need to show that the equilibrium is globally attractive. The derivative of V with respect to time along the trajectory of the system is

$$\begin{aligned}\dot{V} &= m\left(\dot{x} - \frac{x_1}{x}\dot{x} + \dot{y} - \frac{y_1}{y}\dot{y}\right) + \tilde{m}\left(\dot{w} + \frac{1}{q}\dot{z}\right)\\ &= m\left(\lambda + \frac{ad}{\beta} - \left(dx + \frac{\lambda a}{\beta x}\right) + \left(\lambda - \frac{ad}{\beta}\right) - \frac{\lambda\beta - ad}{a}x - pyz + \frac{\lambda\beta - ad}{a\beta}pz\right) + \tilde{m}(cyw - bw - hz)\\ &= -m\lambda\left(\frac{x_1}{x} + \frac{x}{x_1} - 2\right)^2 - (\tilde{m}h + mp(y - y_1))z + \tilde{m}c\left(y - \frac{b}{c}\right)w\\ &= -\frac{m\lambda}{xx_1}(x - x_1)^2 - (\tilde{m}h + mp(y - y_1))z + \tilde{m}c\left(y - \frac{b}{c}\right)w.\end{aligned}$$

First, suppose $y > y_1$ and we choose $m \gg \tilde{m}$, then $\dot{V} < 0$. This result implies that the trajectory enters the region bounded by $y < y_1 + \epsilon$ at some finite time $T_1 > 0$ and then it will stay in this region for $t \in [T_1, \infty)$. Noticing that

$$\begin{aligned}\frac{b}{cQ} - y_1 &= \frac{b}{cQ} - \frac{\lambda\beta - ad}{a\beta}\\ &= \frac{d}{\beta}\left(1 + \frac{b\beta}{cdQ} - \frac{\lambda\beta}{ad}\right)\\ &= \frac{d}{\beta}(R_1 - R_0)\\ &> 0 \quad \text{for } 1 < R_0 < R_1,\end{aligned}$$

we can always select the appropriate m and $\tilde{m}$ to ensure that $b/cQ > y_1 > y - \varepsilon$, i.e., $y < b/cQ + \varepsilon$ for arbitrary small ε. Hence, at some finite time $T > T_1$, the solution must enter $y \le b/cQ$ and stay in this region for $t \in [T, \infty)$.

Having shown that y must be bounded above by b/cQ in finite time, we now proceed to prove that the solution trajectory will approach E_1 asymptotically. Using the inequality in (11), we have

$$bw^\infty \le c(1 - q)y^\infty w^\infty \quad \text{or} \quad \left(\frac{b}{cQ} - y^\infty\right)w^\infty \le 0. \tag{14}$$

For $t \in [T, \infty)$, (14) will only hold if $w^\infty = 0$. Asymptotically, system (3) has the same dynamics as

$$\begin{aligned}\dot{x} &= \lambda - dx - \beta xy\\ \dot{y} &= \beta xy - ay\end{aligned} \tag{15}$$

and this subsystem has two equilibria at

$$\hat{E}_0 = \left(\frac{\lambda}{d}, 0\right) \quad \text{and} \quad \hat{E}_1\,(x_1, y_1)\,.$$

It can be easily verified that when $1 < R_0 < R_1$, subsystem (15) is unstable at $\hat{E}_0$ and locally stable at $\hat{E}_1$. Applying the Lyapunov stability theory to the subsystem, we choose the Lyapunov function as

$$\hat{V}(x, y) = m\left(x - x_1 - x_1 \ln\frac{x}{x_1} + y - y_1 - \ln\frac{y}{y_1}\right).$$

Then

$$\dot{\hat{V}} = -\frac{\lambda}{xx_1}(x - x_1)^2 < 0,$$

for $x \ne x_1$. For $1 < R_0 < R_1$, subsystem (15) is globally asymptotically stable at $\hat{E}_1$ implying that the equilibrium E_1 of system (3) is globally asymptotically stable. □

4. Stability of E_2 and Hopf bifurcation

4.1. Infectious equilibrium with CTL response E_2

As R_0 increases and passes R_1, E_1 becomes unstable and the system moves to the third equilibrium E_2. By Eq. (7), we obtain the characteristic equation at E_2:

$$\Lambda_{E_2}(s) = \det[\lambda I - J(E_2)] = s^4 + \alpha_1 s^3 + \alpha_2 s^2 + \alpha_3 s + \alpha_4,$$

where

$$\alpha_1 = dR_1 + h,$$
$$\alpha_2 = ad\frac{R_0}{R_1}(R_1 - 1) + h\left[dR_1 + a\left(\frac{R_0}{R_1} - 1\right)\right],$$
$$\alpha_3 = ah\left[(b + dR_1)\left(\frac{R_0}{R_1} - 1\right) + d\frac{R_0}{R_1}(R_1 - 1)\right],$$
$$\text{and} \quad \alpha_4 = abdh(R_0 - R_1).$$

It is clear that all $\alpha_i > 0,\ i = 1, 2, 3, 4$ due to $R_0 > R_1 > 1$.

Unlike the previous characteristic polynomials at other equilibria, Λ_{E_2} cannot be factored into polynomials of lesser degree. Hence, local stability of this equilibrium cannot be as easily identified. Instead, we will use the Routh–Hurwitz criterion to analyze its local stability. The criterion states that the corresponding equilibrium is locally asymptotically stable if and only if all the Hurwitz determinants of the characteristic polynomial are positive [15]. For a four dimensional system, the relevant Hurwitz determinants are

$$\Delta_1 = \alpha_1,$$
$$\Delta_2 = \alpha_1\alpha_2 - \alpha_3,$$
$$\Delta_3 = \alpha_3\Delta_2 - \alpha_1^2\alpha_4,$$
$$\text{and} \quad \Delta_4 = \alpha_4\Delta_3.$$

Moreover, Δ_2 and Δ_3 can be written more explicitly as

$$\Delta_2 = A_2(h - b)^2 + B_2(h - b) + C_2,$$
$$\Delta_3 = ah\big[A_3(h - b)^2 + B_3(h - b) + C_3\big],$$

where

$$\begin{aligned}
A_2 &= a\left(\frac{R_0}{R_1} - 1\right) + dR_1,\\
B_2 &= ab\left(\frac{R_0}{R_1} - 1\right) + d(2b + dR_1)R_1,\\
C_2 &= d\left[b(b + dR_1)R_1 + adR_0(R_1 - 1)\right],\\
A_3 &= a(b + dR_1)\left(\frac{R_0}{R_1} - 1\right)^2 + d^2R_1(R_0 - R_1) + d^2R_0(R_1 - 1) + ad\frac{R_0}{R_1}(R_1 - 1)\left(\frac{R_0}{R_1} - 1\right),\\
B_3 &= (b + dR_1)\left[ab\left(\frac{R_0}{R_1} - 1\right)^2 + d^2R_1(R_0 - R_1) + d^2R_0(R_1 - 1)\right] + bd\frac{R_0}{R_1}(R_1 - 1)\left[a\left(\frac{R_0}{R_1} - 1\right) + dR_1\right],\\
C_3 &= d^2\frac{R_0}{R_1}(R_1 - 1)\left[(b + dR_1)\left[a(R_0 - R_1) + bR_1\right] + adR_0(R_1 - 1)\right].
\end{aligned} \tag{16}$$

It is easy to see that all the coefficients A_i, B_i and C_i are positive for any parameter values, since $R_0 > R_1 > 1$ for this case. Therefore, $\Delta_2 > 0,\ \Delta_3 > 0$ as long as $h > b$. In other words, the infectious equilibrium with CTL response, E_2, is always stable if the death rate of the CTLe is higher than that of the CTLp.

In order to obtain more precise stability conditions for the infectious equilibrium with CTL response E_2, we first prove the following lemma to show that if both Δ_2 and Δ_3 can become zero (requiring $h < b$); then Δ_3 will cross zero before Δ_2 does.

Lemma 3. *For $R_0 > R_1$, Δ_2 is positive when Δ_3 crosses zero for some change in parameters.*

Proof. Suppose $\Delta_3 = 0$, then we can rewrite the expression as

$$\Delta_2 = \frac{\alpha_1^2\alpha_4}{\alpha_3}.$$

Since each α_i is positive as long as $R_0 > R_1$, we have $\Delta_2 > 0$. On the other hand, suppose $\Delta_2 = 0$, then we have $\Delta_3 = -\alpha_1^2\alpha_4 < 0$. The proof is complete. □

Thus, to consider the stability E_2, we only need to consider the possibility of $\Delta_3 = 0$.

Now, let

$$\Delta = B_3^2 - 4A_3C_3, \qquad h^* = b - \frac{B_3}{2A_3},$$

$$h_1^* = b - \frac{B_3 + \sqrt{\Delta}}{2A_3} \quad (\Delta > 0), \quad \text{and} \quad h_2^* = b - \frac{B_3 - \sqrt{\Delta}}{2A_3} \quad (\Delta > 0).$$

It is easy to see that $h_1^* < h^* < h_2^* < b$. Then, we have the following theorem.

Theorem 4. *The stability of the infectious equilibrium with CTL response E_2 belongs to one of the following cases:*

(i) *when $\Delta < 0$, E_2 is always stable;*
(ii) *when $\Delta = 0$, E_2 is always stable if $h^* \le 0$; or is stable for $h \in (0, h^*) \cup (h^*, \infty)$ if $h^* > 0$;*
(iii) *when $\Delta > 0$, E_2 is always stable if $h_2^* \le 0$, or is stable for $h \in (h_2^*, \infty)$ if $h_2^* > 0 > h_1^*$, or is stable for $h \in (0, h_1^*) \cup (h_2^*, \infty)$ if $h_1^* > 0$.*

Proof. The proof is straightforward by considering the sign of the quadratic polynomial $A_3(h-b)^2 + B_3(h-b) + C_3$, and thus the details are omitted here for brevity. □

4.2. Hopf bifurcation analysis

In the previous sections, we showed that, as R_0 increases, E_0 loses its stability and transitions to E_1. As R_0 further increases, E_1 would also lose its stability and go to E_2. In this section, we will show that Hopf bifurcation can occur from E_2 if R_0 increases even further with other conditions on the parameter h. Bifurcations are usually determined by the eigenvalues of the Jacobian matrix, but they are often difficult to determine explicitly for high dimensional systems. The next theorem states the necessary and sufficient condition for finding Hopf critical point without finding the eigenvalues and its proof can be found in [10].

Theorem 5. *For $x \in \mathbb{R}^n$, $\mu \in \mathbb{R}$, and $f : \mathbb{R}^n \times \mathbb{R} \to \mathbb{R}^n$, assume that the general nonlinear ordinary differential system*

$$\dot{x} = f(x, \mu)$$

has a locally asymptotically stable equilibrium. The necessary and sufficient condition for a Hopf bifurcation to occur from the equilibrium is

$$\Delta_{n-1} = 0,$$

with α_n and $\Delta_i > 0$, where $1 \le i \le n-2$.

For the present study, this theorem implies that a Hopf bifurcation from E_2 would occur when Δ_3 crosses from the positive to the negative and at the same time, $\Delta_1 > 0$ and $\Delta_2 > 0$ hold. From Lemma 3, we know that the only possible bifurcation which can occur from the infectious equilibrium with CTL response E_2 is a Hopf bifurcation and it may only occur if $h < b$. In particular, we have the following theorem.

Theorem 6. *Let R_H denote the Hopf critical point. Then,*

(i) *when $\Delta < 0$, $R_H = \infty$, that is, there is no Hopf bifurcation;*
(ii) *when $\Delta = 0$, $R_H = \infty$ if the corresponding $h^* \le 0$, or R_H is finite if the corresponding $h^* > 0$ (which only gives a single value for E_2 unstable); so there is no Hopf bifurcation;*
(iii) *when $\Delta > 0$, $R_H = \infty$ if the corresponding $h_2^* \le 0$, giving no Hopf bifurcation, or there is one finite critical value R_H if the corresponding $h_2^* > 0 > h_1^*$, giving rise to a Hopf bifurcation, or there are two finite critical values R_{H_1} and R_{H_2} if the corresponding $h_1^* > 0$, giving rise to two Hopf bifurcations.*

Proof. $\Delta_3 = 0$ is equivalent to find the roots of the quadratic polynomial equation $A_3(h-b)^2 - B_3(h-b) + C_3 = 0$, where all the three coefficients are positive and do not contain h. It is clear that when $\Delta = B_3^2 - 4A_3C_3 < 0$, the quadratic polynomial is positive for any positive parameter values, and thus E_2 is always stable, implying that there is no Hopf bifurcation and so the Hopf critical point is $R_H = \infty$. When $\Delta = 0$, the quadratic polynomial equation has one root

$$h - b = -\frac{B_3}{2A_3}, \quad \text{or} \quad h = b - \frac{B_3}{2A_3} \equiv h^* \quad \text{for } h > 0.$$

So if $h^* \le 0$, then E_2 is always stable because $h > 0$ and no Hopf bifurcation can occur. If $0 < h^* < b$, we have a positive solution for h, and E_2 is stable except for the point $h = h^*$. Thus, the corresponding R_H is a isolated point, that is, except for this point, E_2 is always stable. Thus, for $\Delta = 0$, generically there is no Hopf bifurcation. Finally, for $\Delta > 0$, it may have three possibilities. The roots of the quadratic polynomial for this case is given by

$$h - b = \frac{B_3 \mp \sqrt{\Delta}}{2A_3}, \quad \text{or} \quad h = b - \frac{B_3 \pm \sqrt{\Delta}}{2A_3} \equiv h_{1,2}^* \quad \text{for } h > 0.$$

If $h_1^* < h_2^* \le 0$, E_2 is always stable (i.e. $R_H = \infty$); if $h_2^* > 0 > h_1^*$, then E_2 is stable for $h > h_2^*$ and there is a Hopf bifurcation emerging from the point $h = h_2^*$ with a finite R_H; if $h_1^* > 0$, then E_2 is stable for $h \in (0, h_1^*) \cup (h_2^*, \infty)$, and there are two Hopf bifurcations, which happen at the critical point $h = h_1^*$ and $h = h_2^*$ (the corresponding values in terms of R_0 equal R_{H_1} and R_{H_2}).

To verify if it is possible to have $\Delta = 0$, rewrite Δ as

$$\Delta = \frac{\left\{R_1(dR_1+b) - R_0\left[d(2R_1-1)+b\right]\right\}^2}{d^2R_1^4}\Big\{b^2d^2R_1^2a^2 - 2dR_1\Big[bd^3R_1^3 + \beta\lambda\Big(-2d(R_1-1)+b^2\Big)\Big]a$$
$$+ d^6R_1^6 + 2\beta\lambda d^3R_1^3\Big[b - 2d(R_1-1)\Big] + \beta^2\lambda^2\Big[b^2 - 4d^2(R_1-1)R_1\Big]\Big\}.$$

Since R_1 does not contain a, we can solve the above equation $\Delta = 0$ to find a expressed in terms of other parameters. The first factor gives

$$a = \frac{\lambda\beta\left[d(2R_1-1)+b\right]}{dR_1(dR_1+b)},$$

and the second quadratic polynomial of a yields

$$a = dR_1\left\{bd^3R_1^3 + \beta\lambda\left[-2d(R_1-1)+b^2\right]\right\} \pm 2d^3R_1^2\sqrt{\lambda\beta(R_1-1)\left[\lambda\beta(R_1-1) - bR_1(dR_1-b)\right]}.$$

The above expressions show that all the three cases $\Delta < 0$, $\Delta = 0$ and $\Delta > 0$ are possible. □

The next step is to study the stability of the limit cycles generated from the Hopf bifurcations. To achieve this, consider the general system

$$\dot{\mathbf{X}} = J\mathbf{X} + F(\mathbf{X}), \quad \mathbf{X} \in \mathbb{R}^n,$$

where $J\mathbf{X}$ is the linear part of the system. We first need to find the differential equations' center manifold and then reduce the system to its normal form. Without loss of generality, we assume that $\mathbf{X} = \mathbf{0}$ is the fixed point of interest for the system.

Suppose J has n_c eigenvalues with zero real-part and n_s eigenvalues with negative real-part and $n = n_c + n_s$. Using the eigenvectors of J to form a transformation matrix, the system can be rewritten in block matrix form as

$$\begin{aligned}\dot{\mathbf{x}}_c &= A\mathbf{x}_c + f(\mathbf{x}_c, \mathbf{x}_s)\\ \dot{\mathbf{x}}_s &= B\mathbf{x}_s + g(\mathbf{x}_c, \mathbf{x}_s)\end{aligned} \quad (\mathbf{x}_c, \mathbf{x}_s) \in \mathbb{R}^{n_c} \times \mathbb{R}^{n_s}, \tag{17}$$

where $A \in \mathbb{R}^{n_c \times n_c}$ and $B \in \mathbb{R}^{n_s \times n_s}$. With the eigenvalues of zero real-part, the Center Manifold Theorem [16] guarantees that there exists a smooth manifold $W_c = \{(\mathbf{x}_c, \mathbf{x}_s) | \mathbf{x}_s = q(\mathbf{x}_c)\}$ near the equilibrium point such that the local behavior in the center direction of the system is qualitatively the same as that on the manifold. By differentiating $\mathbf{x}_s = q(\mathbf{x}_c)$, we get $\dot{\mathbf{x}}_s = Dq(\mathbf{x}_c)\dot{\mathbf{x}}_c$. Substituting (17) into the previous identity and rearranging the equation, we get

$$Dg(\mathbf{x}_c)[A\mathbf{x}_c + f(\mathbf{x}_c, q(\mathbf{x}_c))] - Bg(\mathbf{x}_c) - g(\mathbf{x}_c, q(\mathbf{x}_c)) = 0. \tag{18}$$

By solving for $q(\mathbf{x}_c)$, we get a function describing the center manifold. In general, $q(\mathbf{x}_c)$ cannot be solved explicitly. Instead, substituting a Taylor expansion $q(\mathbf{x}_c) = a\mathbf{x}^2 + b\mathbf{x}^3 + \mathcal{O}(\mathbf{x}^4)$ into (18), we can find the coefficients for the expansion by balancing the lower order terms. Based on $q(\mathbf{x}_c)$, we now have a system in the reduced form:

$$\dot{\mathbf{x}}_c = A\mathbf{x}_c + f(\mathbf{x}_c, q(\mathbf{x}_c)).$$

Now that we have the system reduced to the center manifold, we will find the normal form of the system associated with the Hopf bifurcation. To transform the reduced system, we use nonlinear functions $\mathbf{x}_c = \mathbf{y} + h_i(\mathbf{y})$, where each $h_i(\mathbf{y})$ is an ith-degree homogeneous polynomial ($2 \le i \le s$). Given that we are interested in Hopf bifurcation in this paper, we assume that $n_c = 2$ and $\mathbf{x}_c, \mathbf{y} \in \mathbb{R}^2$. Then the system can be transformed to

$$\dot{\mathbf{y}} = A\mathbf{y} + f_2(\mathbf{y}) + f_3(\mathbf{y}) + \cdots + f_s(\mathbf{y}) + DAh_s(\mathbf{y}) - Dh_sA(\mathbf{y}) + \mathcal{O}(|\mathbf{y}|^{s+1}),$$

where $f_i(\mathbf{y})$ represents the ith order terms in the expansion for the function f. We can choose the functions h_s such that $f_s(\mathbf{y}) = Dh_sA(\mathbf{y}) - DAh_s(\mathbf{y})$. Essential terms must remain regardless of our choice of h_s [16]. Hence, we can simplify the system up to a finite degree of terms by applying the process repeatedly. After a simplification up to third order, the normal form of a system associated with a Hopf bifurcation is

$$\begin{pmatrix}\dot{y}_1\\ \dot{y}_2\end{pmatrix} = \begin{pmatrix}(\nu_0\mu + \nu_1(y_1^2+y_2^2))y_1 - (\omega + \tau_0\mu + \tau_1(y_1^2+y_2^2))y_2\\ (\omega + \tau_0\mu + \tau_1(y_1^2+y_2^2))y_1 + (\nu_0\mu + \nu_1(y_1^2+y_2^2))\end{pmatrix} + \mathcal{O}(|\mathbf{y}|^5).$$

We transform these two equations to the polar coordinates as

$$\begin{aligned}\dot{r} &= r(\nu_0\mu + \nu_1 r^2) + \mathcal{O}(r^5)\\ \dot{\theta} &= \omega_0 + \tau_0\mu + \tau_1 r^2 + \mathcal{O}(r^4),\end{aligned} \tag{19}$$

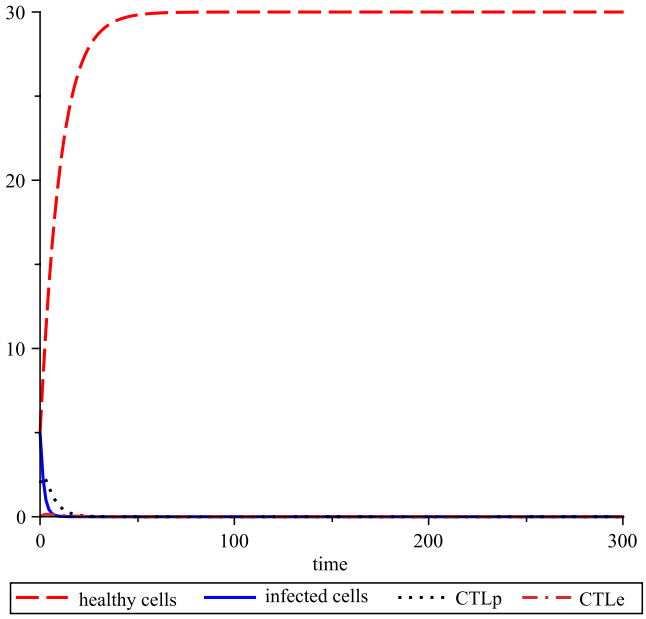

Fig. 1. Simulation of system (3) at $\lambda = 3$.

where r describes the amplitude and θ represents the phase of the periodic motion. By constructing a Poincaré map of the polar coordinate system, one can show that the bifurcating limit cycle is asymptotically stable when $\nu_1 < 0$ and unstable when $\nu_1 > 0$.

We have described a classical approach to determining the stability of Hopf bifurcation here. In order to perform the series of transformations for finding the relevant coefficients, we must first determine the analytic expressions of the eigenvectors for the Jacobian to diagonalize it. We have not been successful in finding these expressions, thus we will not be able to determine the stability of the Hopf bifurcation found in Theorem 6 analytically. An alternative numerical method based on perturbation expansion is described in [17] and we use the associated algorithm to investigate stability for our system in the next section.

5. Numerical simulation

In this section, we demonstrate the analytic results in the previous sections through numerical simulations. To show that the system undergoes qualitative changes as R_0 increases, we vary R_0 by increasing λ and fix the rest of the parameters. The parameter values are chosen as

$$\beta = \frac{3}{400}, \qquad d = c = h = q = \frac{1}{10}, \qquad b = \frac{1}{5}, \qquad a = \frac{1}{2}, \quad \text{and} \quad p = 1.$$

Their selections are biologically realistic and are based on [7,18] and the references therein. With these parameter values, we have

$$R_0 = \frac{3}{20}\lambda \quad \text{and} \quad R_1 = \frac{7}{6}.$$

5.1. Infection-free equilibrium E_0

For $0 < \lambda < \frac{20}{3} \triangleq \lambda_1^c$, $R_0 < 1$. Let $\lambda = 3$, then $R_0 = \frac{9}{20}$. Analytic expression for E_0 is stated in (4). As stated in Theorem 1, E_0 is globally asymptotically stable at these values. At the chosen parameters, the equilibrium values are $(x, y, w, z) = (30, 0, 0, 0)$. Numerical simulation for infection-free equilibrium E_0 is shown in Fig. 1 and it shows that the healthy cells settle to the expected equilibrium value and all other populations die out after a brief period of time.

5.2. Infectious equilibrium without CTL response E_1

Increasing λ further, R_0 passes one and E_0 loses stability to E_1. According to Theorem 2, E_1 remains asymptotically stable when $1 \le R_0 < R_1$, i.e. $\lambda_1^c = \frac{20}{3} \le \lambda < \frac{70}{9} \triangleq \lambda_2^c$. We choose $\lambda = 7.5$, so that the reproductive number is $R_0 = 1.125$.

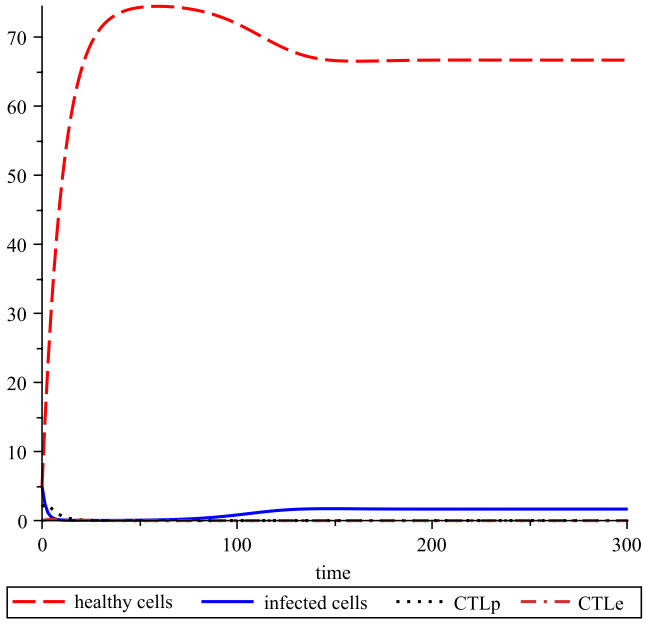

Fig. 2. Simulations of system (3) at $\lambda = 7.5$.

Analytic equilibrium expression for E_1 is shown in (5) and as shown in Fig. 2, the dynamics settle to the numerical values of $(x, y, w, z) = (66.6, 1.16, 0, 0)$. The healthy cell population decreased from the previous equilibrium and at the same time, the infected population increased. As expected from the analytic analysis, the simulation shows that there is no CTL response.

5.3. Infectious equilibrium with CTL response E_2

When R_0 increases and passes R_1, E_1 loses its stability and the system is then stable at the third equilibrium E_2. The reproductive number will be greater than R_1 when $\lambda > 70/9$. Local stability conditions for this equilibrium were shown in Theorem 4 using the Routh–Hurwitz stability theorem. Hence, we shall check the conditions for the theorem numerically. Using the selected parameters, the characteristic equation in terms of λ is

$$\Lambda_{E_2}(s) = s^4 + \frac{13}{60}s^3 + \left(\frac{3\lambda}{400} - \frac{23}{600}\right)s^2 + \left(\frac{3\lambda}{1400} - \frac{19}{1200}\right)s + \left(\frac{3\lambda}{20\,000} - \frac{7}{6000}\right).$$

From the characteristic polynomial, the relevant Hurwitz determinants are

$$\Delta_2(\lambda) = -\frac{29}{56\,000}\lambda + \frac{271}{36\,000},$$

$$\text{and} \quad \Delta_3(\lambda) = -\frac{87}{78\,400\,000}\lambda^2 + \frac{5809}{336\,000\,000}\lambda - \frac{2783}{43\,200\,000}.$$

Solving for λ when $\Delta_3 = 0$, we find that the roots are

$$\lambda_1 = \frac{1610}{261} \approx 6.17 \quad \text{and} \quad \lambda_2 = \frac{847}{90} \approx 9.41. \tag{20}$$

Thus, E_2 is stable when $70/9 < \lambda < 847/90$. We choose $\lambda = 8$. Direct evaluations of Δ_2 and the coefficients of the characteristics polynomial at $\lambda = 8$ show that they are all positive. Hence, we have satisfied the local stability criteria from the Routh–Hurwitz theorem.

According to the formulas given in (16), we have

$$A_3 = \frac{27}{9800}\left[\left(\lambda - \frac{3899}{540}\right)^2 + \frac{115\,199}{291\,600}\right] > 0,$$

$$B_3 = \frac{27}{49\,000}\left[\left(\lambda - \frac{22\,561}{3240}\right)^2 + \frac{12\,175\,079}{10\,497\,600}\right] > 0,$$

$$C_3 = \frac{1}{5\,600\,000}\lambda(30\lambda - 133) > 0 \quad \text{for } \lambda > \frac{70}{9},$$

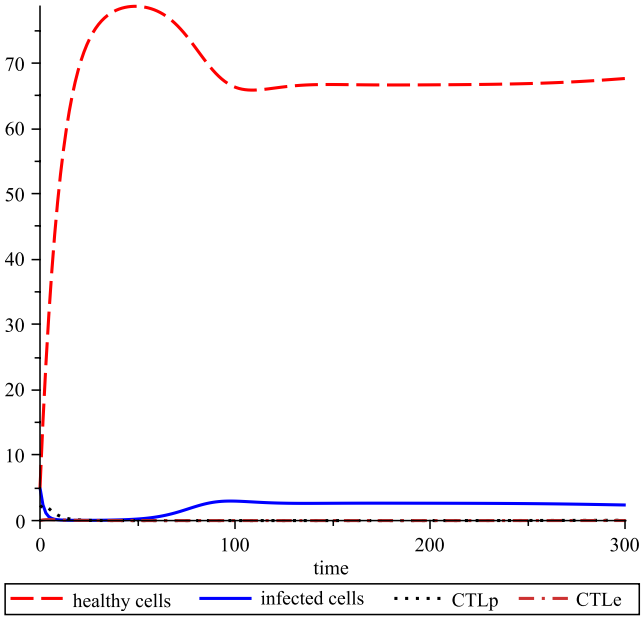

Fig. 3. Simulations of system (3) at $\lambda = 8$.

which yields

$$\Delta = \frac{29}{38\,416\,000\,000}(18\lambda - 133)^2\left[\left(\lambda - \frac{11\,935}{1566}\right)^2 - \frac{1\,250\,921}{613\,089}\right].$$

Hence, $\Delta = 0$ yields

$$\begin{aligned}\lambda &= \frac{11\,935 \pm 98\sqrt{521}}{1566}, \frac{133}{18}, \frac{133}{18}\\ &\approx 6.192917246, 7.388888889, 7.388888889, 9.049739204.\end{aligned}$$

Let $\lambda^* = \frac{11\,935+98\sqrt{521}}{1566} \approx 9.049739204$. Then, $\Delta < 0$ for $\frac{70}{9} < \lambda < \lambda^*$, $\Delta = 0$ for $\lambda = \lambda^*$, and $\Delta > 0$ for $\lambda > \lambda^*$. Therefore, E_2 is always stable for $\frac{70}{9} < \lambda < \lambda^*$. When $\lambda = \lambda^*$, we have $h^* = \frac{2839-25\sqrt{521}}{43\,080} \approx 0.05265469799 > 0$, so E_2 for this numerical example with the given value $h = \frac{1}{10} \neq h^*$ is stable. When $\lambda > \lambda^*$, we have two roots from the quadratic polynomial as

$$h^*_{1,2} = \frac{29\,160\lambda^2 - 436\,086\lambda + 1\,615\,775 \pm 5(18\lambda - 133)\sqrt{84\,564\lambda^2 - 1\,288\,980\lambda + 4\,739\,329}}{(540\lambda - 3899)^2 + 1\,151\,199}.$$

It can be shown that both $h^*_{1,2} > 0$ for $\lambda > \lambda^*$. Thus, according to Theorem 4, we know that E_2 is stable for $(0, h^*_1) \cup (h^*_2, \infty)$. Suppose $\lambda = 9.2$, then $h^*_1 = 0.03181658398$ and $h^*_2 = 0.08247353652$. The given value $h = 0.10 > h^*_2$, implying that E_2 is stable. If we take $\lambda = 10$, then we have $h^*_1 = 0.01728507103$ and $h^*_2 = 0.1270566231$, which indicates that $h = 0.10 \in (h^*_1, h^*_2)$, and so E_2 is unstable.

Based on the analytic equilibrium expression of E_2 given by (6), there should be non-zero CTL responses at this equilibrium. In Fig. 3, the responses of each population settle to the expected equilibrium values of $(x, y, w, z) = (77.14, 2.22, 0.35, 0.8)$.

5.4. Hopf bifurcation

As stated in Theorem 6, there will be a Hopf bifurcation for large enough R_0. By calculations in (20), Δ_3 crosses zero and becomes negative when $\lambda = 847/90$. Hence, Hopf bifurcation occurs at $\lambda_H = 847/90$. Or in terms of reproductive number, we have $R_H = 847/600 \approx 1.4115$. Numerically, the Hurwitz determinants at $R_0 = R_H$ are

$$\Delta_2 = \frac{637}{240\,000}, \quad \text{and} \quad \Delta_3 = 0.$$

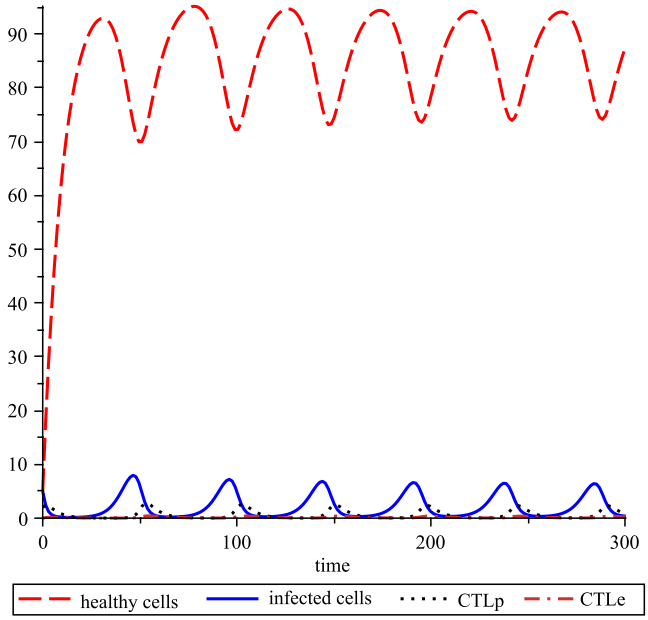

Fig. 4. Simulations of system (3) with oscillations at $\lambda = 10$ ($\mu = 53/90$).

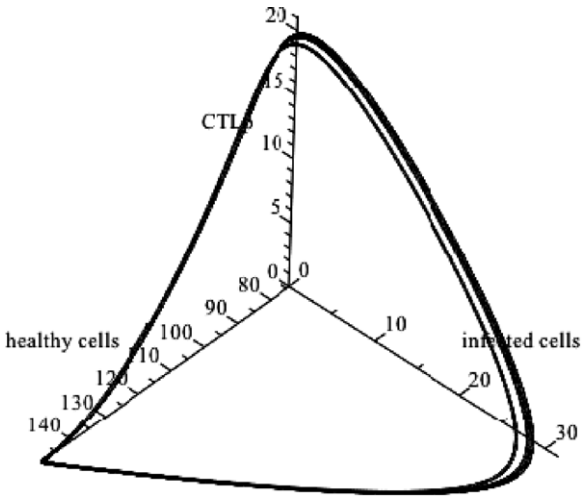

Fig. 5. Limit cycles of system (3) at $\lambda = 10$ ($\mu = 53/90$).

To show that Δ_3 crosses from the positive to the negative, we select $\lambda = 98/10 \approx 9.8$, at which

$$h_1^* = 0.01889876185, \qquad h_2^* = 0.1198979582.$$

For the given value $h = 0.10$, E_2 is unstable and limit cycles bifurcating from the Hopf critical point $R_0 = R_H$. In fact, when $h = 0.10$, the relevant Hurwitz determinants become

$$\Delta_2 = \frac{883}{360\,000}, \quad \text{and} \quad \Delta_3 = -\frac{677}{432\,000\,000}.$$

Comparing the present numeric values to those evaluated earlier, we see that Δ_3 crosses from the positive into the negative nondegenerately. By Theorem 5, one pair of complex conjugate eigenvalues crosses from $\mathbb{C}^-$ into $\mathbb{C}^+$ and Hopf bifurcation occurs. Numerical solutions of the system are plotted in Fig. 4, showing oscillations for each variable. In Fig. 5, a limit cycle between the healthy cells, the infected cells and the CTLp populations is observed in the phase space.

Stability conditions for the periodic solution can be obtained from the method of normal form theory, Lyapunov–Schmidt reduction or Poincaré–Lindstedt expansion. While these methods proceed differently, they all require the explicit expressions for the eigenvalues and the eigenvectors from the Jacobian of the system for analytic calculations. As mentioned earlier, we were unable to obtain the necessary expressions for such analysis, so we turned to a numerical algorithm given

by [19] to investigate the stability of the orbits. This algorithm employs the method of multiple time scale to expand the system in question at a critical Hopf bifurcation point. Solving the perturbed differential equations, one could determine the constants which uniquely determines the normal form of the system.

We use a Maple implementation of the aforementioned algorithm to determine the stability at critical point $R_H = 847/90$. In polar coordinates, the normal form for Hopf bifurcations is described in (19). Applying to our present situation, we have $\mu = \lambda - \lambda_H = 10 - 847/90 = 53/90$. The form is uniquely determined by the constants ν_0, ν_1, ω_0, τ_0 and τ_1. Imaginary component of the bifurcating eigenvalue pair is $\omega_0 = \sqrt{2}/10$. As shown in [8], the other constants are also determined by the Maple implementation from [19] and they are

$$\nu_0 = \frac{8370}{1\,006\,943}, \qquad \nu_1 = -\frac{7\,159\,359\,703\,000}{25\,412\,370\,525\,507},$$
$$\tau_0 = \sqrt{2}\frac{23\,400}{1\,006\,943}, \quad \text{and} \quad \tau_1 = -\frac{724\,938\,191\,405\,000}{76\,237\,111\,576\,521}.$$

Since $\nu_1 < 0$, the bifurcating limit cycles are stable. Other than stability, we can also find the amplitude and frequency of the periodic solutions. Based on the previously deduced parameters, we write the third-order normal form of (3) as

$$\begin{aligned} \dot{r} &= r\left(\frac{8370}{1\,006\,943}\mu - \frac{7\,159\,359\,703\,000}{25\,412\,370\,525\,507}r^2\right), \\ \dot{\theta} &= \frac{\sqrt{2}}{10} + \sqrt{2}\frac{23\,400}{1\,006\,943}\mu - \frac{724\,938\,191\,405\,000}{76\,237\,111\,576\,521}r^2. \end{aligned} \tag{21}$$

By setting the first equation in (21) to zero, the roots are

$$r = 0 \quad \text{and} \quad r = \frac{171}{715\,935\,970\,300}\sqrt{5\,171\,871\,333\,929\,279\mu}. \tag{22}$$

The non-zero root in (22) corresponds to the amplitude of the bifurcation. Furthermore, the frequency of the said solution is given by

$$\omega = \sqrt{2}/10 + \left(\sqrt{2}\frac{23\,400}{1\,006\,943} - \frac{2\,022\,577\,554\,019\,950}{7\,209\,067\,137\,417\,929}\right)\mu.$$

6. Discussion and conclusion

Wodarz et al. built a model in [7] to investigate the interactions between healthy and infected cells as well as primary and secondary CTL response cells. In terms of analytic investigation of the model, the authors only analyzed the structure of the equilibria and some specific cases. For a higher dimension system, equilibrium behavior alone cannot fully describe the full dynamics of the system. Stability and bifurcation analysis are important for the full range of possibilities. In this work, we fully described the stability of the infection-free equilibrium E_0, the infectious equilibrium without CTL response E_1, and the infectious equilibrium with CTL response E_2.

Analytically, we showed that when $0 < R_0 < 1$, the infection-free equilibrium is globally asymptotically stable; when $1 < R_0 < R_1$, the infection-free equilibrium becomes stable and the infectious equilibrium without CTL response is globally asymptotically stable; when $R_1 < R_0 < R_H$, the infectious equilibrium with CTL response may be locally asymptotically stable; finally, given $\Delta > 0$, there exists a Hopf bifurcation from the infectious equilibrium with CTL response for an appropriate choice of the system's parameters. Given that R_0, R_1, R_H, and Δ are comprised of the parameters of the system, we have shown how the parameters effect the dynamics of the model.

From Section 1, we see that system (3) is formed by splitting the CTL class in system (2) into two different response classes. By a direct calculation, one can see that the basic productive number R_0 for systems (2) and (3) are the same. Hence, the parameters in the equations dealing with CTL responses have no effect on R_0. In other words, the dynamics of the CTL responses do not affect the way systems transition from infection free equilibrium to the infectious equilibria. Given that the CTL cells have no role in preventing infections, this aspect of the model is consistent with biological situation.

Originally, the authors of [7] only explored aspects of system (3) numerically. In our analysis, we have identified periodic solutions of the model in a rigorous manner. These sustained oscillations stem from the infectious equilibrium with CTL response. For the immune system, this transition represents a change from homeostatic states to sustained fluctuations of the cell populations in the model. The sustained oscillations from the Hopf bifurcation implies that upon primary infection, the pathogen may not always be cleared entirely with the CTL responses. As one could see from Fig. 4, the number of the infected cells may decrease, but over time, the population oscillates and cannot be completely eradicated. This phenomenon can be viewed as an individual having a chronic disease that may flare up from time to time.

Through the expressions obtained from the stability and bifurcation analysis, we are able to better understand the transition from a homeostatic state to oscillations triggered by a Hopf bifurcation. We showed that $\Delta > 0$ is a necessary condition for Hopf bifurcation in Theorem 6. This condition constrains $h < b$ for sustained oscillations to occur. These two

constants are the decaying rates of the two classes of immune cells. When effectors have longer life span than precursors ($h < b$), flare ups of the disease can occur. On the other hand, when the precursors have longer life span than the effectors ($h > b$), the immune system is able to prevent flare ups and control the system at a steady state. This result, based on expressions obtained from the bifurcation analysis, is in agreement with the analysis [20]. Like system (3), this model of lymphocytic choriomeningitis virus has precursor and effector CTL classes and it also involves time-delay. Both these models predict that the immune system is more efficient in controlling the disease when the precursors outlive the effectors.

Traditionally, immunologists have ignored the oscillatory behavior of the immune system. They considered equilibrium states as the natural states of the immune system and any other behavior, such as oscillations, were seen as transitional states between two equilibria. Studies of the immune system and pathogen interactions show that equilibrium states may not be the only consistent behavior in immune response [21]. To model the sustained oscillations in the aforementioned studies using differential equations, one must look to a model that could incorporate possible Hopf bifurcations. For in-host virus dynamics, models including intra-cellular delay [22,20] and experimental treatment [8] have shown sustained oscillations. In this paper, we showed that, even without time-delay, the dynamics from the interactions of precursors and effectors added to the model of healthy and infected host cells could also produce a Hopf bifurcation. Thus, we have provided another theoretical reason to explain the periodic dynamics in future research.

The interplay between virus and the host immune system is a complicated process, which involves cell production, viral attachment, viral replication and pathogen clearance. While we have shown that oscillatory patterns can be obtained for a wide range of parameters in a model, not all of these patterns are necessarily biologically realistic. Experimental works to confirm such behavior are necessary and essential. With two classes of CTL cells considered, the model is rich with various dynamics. This model maybe improved upon by considering other effects. In future works, different therapeutic options maybe added to understand their effects on CTL productions as well as the overall health of the individual. One may also introduce the delay effects of viral gestation in latently infected cells to provide a more realistic model. These added dynamics are sure to make the mathematical model more challenging to analyze.

References

[1] D. Male, J. Brostoff, D. Roth, I. Roitt, The Journal of Immunology (2006).
[2] M. Nowak, R. May, Virus Dynamics, Oxford University Press, 2000.
[3] D. Wodarz, Killer Cell Dynamics: Mathematical and Computational Approaches to Immunology, Springer Verlag, 2007.
[4] R. Anderson, R. May, Infectious Diseases of Humans: Dynamics and Control, Oxford Univ. Press, 1991.
[5] R. De Boer, A. Perelson, Target cell limited and immune control models of HIV infection: a comparison, Journal of Theoretical Biology 190 (3) (1998) 201–214.
[6] M. Nowak, C. Bangham, Population dynamics of immune responses to persistent viruses, Proceedings of the National Academy of Sciences of the United States of America 85 (1996) 3509.
[7] D. Wodarz, K. Page, R. Arnaout, A. Thomsen, J. Lifson, M. Nowak, A new theory of cytotoxic T-lymphocyte memory: implications for HIV treatment, Philosophical Transactions of the Royal Society B: Biological Sciences 355 (1395) (2000) 329.
[8] X. Jiang, P. Yu, Z. Yuan, X. Zou, Dynamics of an HIV-1 therapy model of fighting a virus with another virus, Journal of Biological Dynamics 3 (4) (2009) 387–409.
[9] C. Egami, Bifurcation analysis of the Nowak–Bangham model in CTL dynamics, Mathematical Biosciences 221 (1) (2009) 33–42.
[10] P. Yu, Closed-form conditions of bifurcation points for general differential equations, International Journal of Bifurcation and Chaos 15 (4) (2005) 1467–1483.
[11] W. Hirsch, H. Hanisch, J. Gabriel, Differential equations models for some parasitic infections: methods for the study of asymptotic behavior, Communications on Pure and Applied Mathematics 38 (1985) 733–753.
[12] H.R. Thieme, Mathematics in Population Biology, Priceton, 2003.
[13] C. Castillo-Chavez, H. Thieme, Asymptotically autonomous epidemic models, in: Mathematical Population Dynamics: Analysis of Heterogeneity, 1995, pp. 33–50.
[14] A. Korobeinikov, Global properties of basic virus dynamics models, Bulletin of Mathematical Biology 66 (4) (2004) 879–883.
[15] A. Pritchard, Mathematical Systems Theory, Springer, 2005.
[16] J. Guckenheimer, P. Holmes, Nonlinear Oscillations, Dynamical Systems, and Bifurcations of Vector Fields, Copernicus, 1990.
[17] P. Yu, K. Huseyin, A perturbation analysis of interactive static and dynamic bifurcations, IEEE Transactions on Automatic Control 33 (1) (1988) 28–41.
[18] Y. Wang, Y. Zhou, J. Wu, J. Heffernan, Oscillatory viral dynamics in a delayed HIV pathogenesis model, Mathematical Biosciences 219 (2) (2009) 104–112.
[19] P. Yu, Computation of normal forms via a perturbation technique, Journal of Sound and Vibration 211 (1) (1998) 19–38.
[20] T. Luzyanina, K. Engelborghs, S. Ehl, P. Klenerman, G. Bocharov, Low level viral persistence after infection with LCMV: a quantitative insight through numerical bifurcation analysis, Mathematical Biosciences (ISSN: 0025-5564) 173 (1) (2001) 1–23.
[21] J. Stark, C. Chan, A. George, Oscillations in the immune system, Immunological Reviews (ISSN: 1600-065X) 216 (1) (2007) 213–231.
[22] R. Culshaw, S. Ruan, G. Webb, A mathematical model of cell-to-cell spread of HIV-1 that includes a time delay, Journal of Mathematical Biology (ISSN: 0303-6812) 46 (5) (2003) 425–444.